Particle & Particle Systems Characterization
www.particle-journal.com

Bioconjugated Core–Shell Microparticles for High-Force Optical Trapping

*Juan Carlos Cordova, Dana N. Reinemann, Daniel J. Laky, William R. Hesse, Sophie K. Tushak, Zane L. Weltman, Kelsea B. Best, Rizia Bardhan, and Matthew J. Lang**

Due to their high spatial resolution and precise application of force, optical traps are widely used to study the mechanics of biomolecules and biopolymers at the single-molecule level. Recently, core–shell particles with optical properties that enhance their trapping ability represent promising candidates for high-force experiments. To fully harness their properties, methods for functionalizing these particles with biocompatible handles are required. Here, a straightforward synthesis is provided for producing functional titania core–shell microparticles with proteins and nucleic acids by adding a silane–thiol chemical group to the shell surface. These particles display higher trap stiffness compared to conventional plastic beads featured in optical tweezers experiments. These core–shell microparticles are also utilized in biophysical assays such as amyloid fiber pulling and actin rupturing to demonstrate their high-force applications. It is anticipated that the functionalized core–shells can be used to probe the mechanics of stable proteins structures that are inaccessible using current trapping techniques.

1. Introduction

Optical traps have been widely used as a tool to measure small displacements, exert finely controlled forces, and manipulate microscopic objects.[1] By tethering a biomolecule of interest between a dielectric particle, for example, a plastic bead and a glass coverslip surface, the optical force and position can be finely controlled to measure the mechanical properties of proteins, nucleic acids, biopolymers, and protein aggregates involved in physiological function as well as disease.[2–5] An optical trap is formed by focusing a laser beam into a diffraction-limited spot using a high numerical aperture objective lens. In the presence of the optical trap, a dielectric particle, through redirecting the light, will experience a gradient force laterally toward the focus of the trap where the photon flux is highest, as well as a scattering force in the direction of propagation of light.[1] A dielectric object, referred to here as a trapping handle, is trappable when the magnitude of the gradient force is larger than that of the scattering force. Using a single gradient optical trap, objects with refractive indices larger than $n = 1.73$ become untrappable in an aqueous medium, such as biological buffers, due to large amounts of scattering.[6] Yet, fine-tuning the difference in index of refraction of the trapping handle and the surrounding medium can lead to higher trapping force.[7]

Micrometer-sized beads, normally made of polystyrene, are widely employed in optical trapping experiments. These beads are commercially available and feature a wide range of surface functionalization with chemically reactive molecules including primary amines, carboxylates, and hydroxyls, which in turn can be conjugated to biomolecules of interest for single-molecule experiments.[8] However, most experiments utilizing these polystyrene beads are measuring relatively low forces, such as from molecular motor motility (≈5 pN)[9] binding affinity of proteins to cytoskeletal filaments (≈50 pN)[10] and structural transitions of DNA (≈65 pN).[11] Conventional optical tweezers have been used to initially probe high-force biological phenomena such as amyloid fiber strength,[3,4] DNA packaging,[12] and rheology of cytoskeletal networks[13] but high-force measurements generally require either larger beads or alternate approaches such as magnetic tweezers,[14,15] microneedle manipulation,[15,16] or atomic force microscopy.[15]

Recently, Schaffer and co-workers developed anatase-titania core microspheres with decreased scattering and exceptionally high trapping stability[17] without the need to use high laser powers that can lead to photodamage of biomolecules, sample heating, and damage to optics.[18] Titania microparticles with an anatase core and amorphous shell represent a model system for high-force optical trapping experiments due to the differences in dielectric constant between the core and shell that allows for a simple assay change (from polystyrene beads to core–shell microparticles) to increase the trap stiffness without altering the instrumental setup. In order to leverage these very promising

Dr. J. C. Cordova, D. N. Reinemann, D. J. Laky, S. K. Tushak, Z. L. Weltman, K. B. Best, Prof. R. Bardhan, Prof. M. J. Lang
Department of Chemical and Biomolecular Engineering
Vanderbilt University
Nashville, TN 37235, USA
E-mail: matt.lang@vanderbilt.edu
Dr. W. R. Hesse
Department of Mechanical and Biological Engineering
Massachusetts Institute of Technology
Cambridge, MA 02139, USA
Prof. M. J. Lang
Department of Molecular Physiology and Biophysics
Vanderbilt University Medical Center
Nashville, TN 37232, USA

DOI: 10.1002/ppsc.201700448

 © 2018 WILEY-VCH Verlag GmbH & Co. KGaA, Weinheim

core–shell titania microparticles for cell and molecular biophysics research, clear and straightforward methods for synthesizing and functionalizing the surface must be developed. Whereas microparticles with an antireflection coating have been preliminarily utilized in cellular binding and manipulation experiments,[19,20] the proteins used for binding were noncovalently attached to the bead surface. Noncovalently tethered biomolecules are not ideal for high-force applications due to uncertainties in the protein geometry and strength.

Here, we report a robust synthetic approach to design core–shell titania microparticles that achieve high trapping forces and a strategy for covalently linking biological components, such as proteins (prion proteins, streptavidin) or nucleic acids, to these particles. We then demonstrate their use in inherently high-force biophysical assays. We anticipate the methods described here will permit wider use of these improved trapping handles in optical trapping applications requiring the use of currently inaccessible high forces,[3,4] as well as in combined coincident optical trapping and fluorescence assays[21,22] where minimizing laser powers while maintaining trapping stability is vital.[23]

2.1. Results and Discussion

2.1.1. Synthesis and Characterization of Core–Shell Particles

Using the synthetic strategy outlined in **Figure 1**, we provide a straightforward method for the synthesis of optical trapping handles with increased trapping stability. Our synthetic approach is considerably modified from work described in the literature and optimized to generate high trapping forces.[25–27] A representative image of the anatase cores is shown in **Figure 2**A. In the initial step, titania cores are synthesized by a nucleation reaction where the diameter of the cores is linearly dependent on the concentration of titanium butoxide (TBT) used (Figure 2B). Using 2–3 $\times$ 10^{-3} M TBT, we were able to synthesize cores with tightly controlled diameters between 400 and 800 nm. To determine the size of the particles, we found that particle diameters estimated using a scanning electron microscope (SEM) agreed well with measurements (normally less than 10% error) using a custom-built light microscope equipped with a 100× objective (1.4 numerical aperture Nikon) and differential interference contrast microscopy (DIC). To calculate particle diameters, DIC images were used to measure the average diameter of a particular particle in pixels using the software ImageJ. With a predetermined pixel size of 23.75 nm pixel^{-1} for the CCD camera used (DAGE-MTI), we estimated the average diameter in nanometers for numerous beads per condition.

Since a mismatch in the index of refraction between the core ($n = 2.3$)[26] and shell ($1.6 < n < 1.8$)[26] materials is vital for enhanced trapping stability,[17] Raman spectroscopy was utilized to confirm the anatase phase of the cores after calcination. Raman spectra show the emergence of the characteristic peaks for anatase at 399, 519, and 639 cm^{-1}[41,42] only upon heating the cores at 500 °C (Figure 2C, red).

Coating of the anatase cores with amorphous titania shells was carried out at constant surfactant concentration, using varying concentrations of TBT precursor to dictate the shell thickness (Figure 2D). Previously, it had been suggested that a silica layer deposited on the surface of core–shells could provide a conjugation strategy to couple molecules of interest to the particles but was mainly used as a way to generate fluorophore-free luminescent beads upon calcination.[26,27] However, silica coating of particles can be a tedious reaction and often leads to particle agglomeration and loss of functionality.[28] Instead, we employed a silane functionalizer, (3-mercaptopropyl)trimethoxysilane (MPTS), to incorporate thiol groups on the titania shell surface. Although thiol chemistry provides a convenient strategy for coupling to primary amines in biomolecules, other silane analogues can easily be used to enable different surface chemistries including amines and hydroxyls.

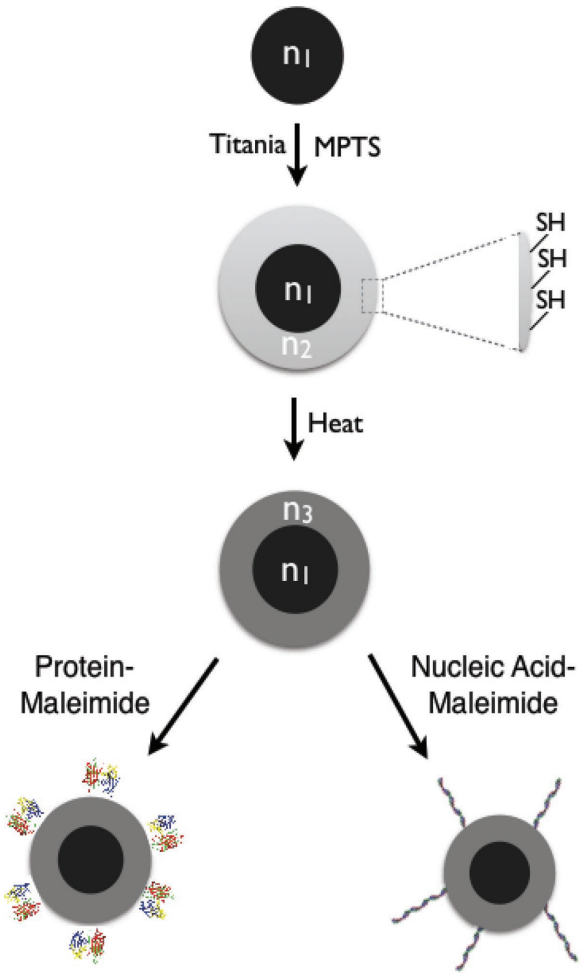

Figure 1. Synthetic strategy for the production of anatase-titania core–shell particles functionalized with proteins or nucleic acid structures. Anatase cores with a high index of refraction ($n_1 \approx 2.3$) are coated with an amorphous titania shell (with index of refraction $n_2 \approx 1.6$), and functionalized with surface-exposed thiol groups using MPTS (see the Experimental Section). The index of refraction of the shell can be tuned by heating to an estimated $n_3 \approx 1.7$–1.8, which leads to high trapping stability (see Discussion). The surface-exposed thiol groups can be cross-linked to proteins and nucleic acids using thiol chemistry.[24]

© 2018 WILEY-VCH Verlag GmbH & Co. KGaA, Weinheim

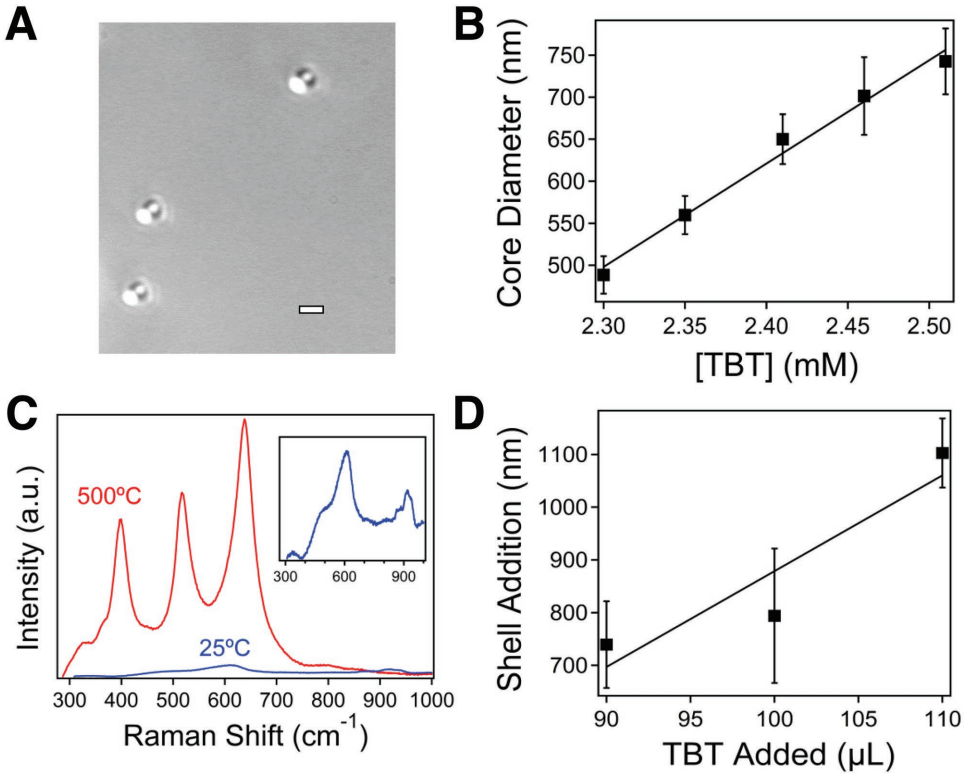

Figure 2. Synthesis and characterization of core–shell particles. A) Image of anatase cores (scale bar, 500 nm) obtained using a light microscope with DIC. B) Anatase core size increases with additional TBT utilized (avg. ± std., $N = 30$ per concentration measured). C) Raman spectra for cores before (blue) and after (red) calcination showing the transition of titania to the anatase phase, seen as appearance of bands described in the text. D) Size of shell thickness using different amounts of TBT in the reaction with no heating (avg. ± std., $N = 10$ per concentration measured).

2.1.2. Particle Size and Trapping Stability are Temperature Dependent

The amorphous titania shell has an index of refraction of ≈1.55 which is lower than the suggested $n = 1.75$ for optimal trapping stability of the core–shell microparticles, as predicted by theory.[17] The index of refraction of titania, and concomitantly the size of the microparticle, can be tuned by heating. Upon heating at 50 °C, the particle diameter decreased ≈15% within 15 min (**Figure 3**A). Thus, to synthesize core–shells with a final diameter of 0.9–1.1 µm we started with core–shells ≈1.3 µm in diameter prior to heating. Using optical tweezers, we characterized the trapping stability of the particles by comparing the trap stiffness at a constant laser power (≈370 mW at 1064 nm before the objective), between the core–shell microparticles, and commercially available polystyrene beads of a similar size (1.025 µm, $n = 1.57$, Spherotech).

Polystyrene beads are the current gold standard in the field of single-molecule biophysics for optical trapping experiments, including at high forces.[3] We demonstrate here that our core–shell microparticles displayed higher trapping stiffness than the polystyrene beads, even in the absence of heating (Figure 3B).

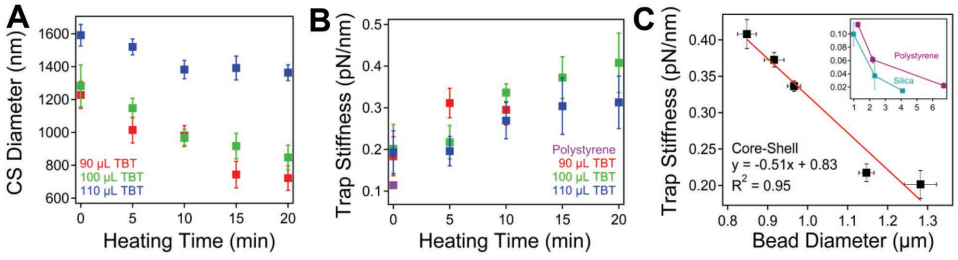

Figure 3. Temperature dependence of core–shell particles. A) Average diameter of anatase-titania core–shell particles as a function of heating time at 50 °C. Three separate batches of core–shells are plotted, with initial diameters ranging from 1.6 to 1.2 µm, depending on the amount of TBT used (avg. ± std., $N = 10$ particles per heating measurement). B) Average trapping stiffness for conventional polystyrene beads (P.S., diameter ≈ 1.25 µm), and core–shells heated up to 20 min (avg. ± std., $N = 10$ particles per stiffness measurement). C) Trap stiffness versus core–shell diameter correlation for 100 µL TBT. Inset: Trap stiffness (avg ± std., $N = 10$ particles per measurement) of polystyrene (Spherotech) and silica (Bangs Labs) beads of different diameters.

© 2018 WILEY-VCH Verlag GmbH & Co. KGaA, Weinheim

Upon heating, the change in density of the titania shell leads to an increase in the index of diffraction,[26] and we observe a 3–4 times increase in trap stiffness for the core shells (Figure 3B). When heated for longer than 20 min, the core–shells were no longer trappable with a single beam trap, likely due to an increase in the scattering force.[17] These results demonstrate functionalized anatase-titania core–shell particles feature up to a fourfold improvement in trapping stability compared to standard polystyrene beads.

There is a linear correlation between trap stiffness and core–shell bead diameter (also associated with increased refractive index change with increased heating time, Figure 3C). For comparison, the trap stiffnesses of different sized polystyrene (1.09, 2.192, and 6.7 μm; Spherotech) and silica (0.97, 2.32, and 4.09 μm; Bangs Labs) were also measured (Figure 3C inset). The trap stiffness measurements are much lower than for our core–shell microparticles, and the stiffness decreases with increasing bead diameter. Here, we note that the correlation between bead diameter (d_{bead}) and trap stiffness is complex due to the measured bead sizes falling within different optic regimes. Most optical trapping applications fall into an intermediate regime ($d_{bead} \approx \lambda_{trap}$, here λ_{trap} = 1064 nm) between Rayleigh ($d_{bead} \ll \lambda_{trap}$) and Mie ($d_{bead} \gg \lambda_{trap}$) scattering conditions.[1,29] As d_{bead} becomes greater than λ_{trap}, the trapping rays are spread out over a larger distance, causing a decrease in stiffness with increased d_{bead}.[1,29,30] These results stress the importance of finely tuning the core–shell microparticle diameter and their overall improvement over conventional beads.

2.1.3. Biophysical Experiments Using Core–Shell Particles

Since the core–shell microparticles surpassed the standard polystyrene beads in trapping stability, we then functionalized the microparticles with proteins to pursue two different high-force assays. First, we coupled core–shell particles to the prion protein Sup35 labeled with an Alexa555 fluorescent tag. We chose to use the Sup35 protein, produced in *Saccharomyces cerevisiae*, due to its involvement in amyloid fibril formation.[3] As demonstrated by Dong et al. and Castro et al., single amyloid fibers, which form aggregates in neurodegenerative diseases such as Alzheimer's, have a shockingly large modulus, greater than that of spider silk.[3,4] Amyloid fiber stability and strength have been of interest to the biophysics and medical fields investigating mechanisms of prion diseases.[31] In the study by Dong et al., an optical trap was used to unfold and rupture amyloid fibers. However, a conventional optical trap required a denaturing reagent to rupture fibers.[3] The core–shell particles synthesized in this study are well suited for this experiment that requires greater force than previously attained.

Here, we used sulfosuccinimidyl 4-[N-maleimidomethyl] cyclohexane-1-carboxylate (sulfo-SMCC) to covalently cross-link the amine-terminus of Sup35 NM protein (N-terminal and middle domains) fluorescently labeled with Alexa555 to surface-exposed thiol groups on the core–shells. Sup35-coated core–shells were imaged using DIC and total internal reflection fluorescence (TIRF) microscopy (**Figure 4**A–C). Fluorescence intensity of the core–shells decreased with time due to photobleaching of the Alexa555 dye, suggesting the Sup35 protein successfully

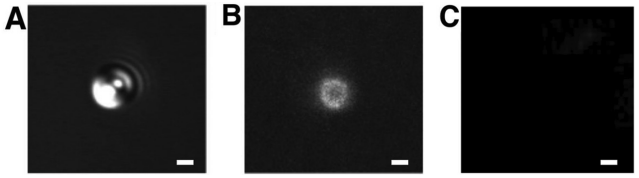

Figure 4. Fluorophore addition to core–shell particles. A) DIC image of anatase-titania core–shell particles coated with Sup35 proteins. B) TIRF microscopy images show fluorescence emission of the Alexa555 dye on the surface-bound Sup35 protein. The fluorescence intensity from the beads decreased with time due to photobleaching of the dye. C) Fluorescence image of streptavidin coated core-shell particle with no dye. No autofluorescence was observed. Scale bar: 500 nm.

bound the core–shell surface. The same process was successfully carried out to covalently bind streptavidin to the core–shell surface. Given the ubiquitous use of biotinylated proteins, nucleic acids, and molecular motors in single-molecule experiments, streptavidin-coated core–shells can be easily introduced into well-developed assays to probe biomolecule mechanics and activity (e.g., ClpXP mechanical protein degradation,[32] protein folding–unfolding[33]).

We performed a surface-tethered amyloid fiber assay using our core–shell titania microparticles functionalized with streptavidin and subsequently conjugated with biotinylated NM monomer (see the Experimental Section). A schematic of the assay is shown in **Figure 5**A. Upon the sequential bottom-up assembly of core–shell fiber tethers, a piezostage was translated against a trapped bead to elongate and concomitantly impart force on the fiber (Figure 5B). As the microparticle is pulled away from the focus of the optical trap, the force across the fiber is above 100 pN, and multiple domains of the fiber unfold. This leads to sharp decreases in bead position as the bead moves closer to the trap center (Figure 5C). This lessens the force on the fiber continually until no more events are observed at the end of the trace. The same tether was pulled again (Figure 5D), and as a significant amount of force is imparted on the partially unfolded fiber, complete rupture is observed. Evidence of this was found by a clean rupture to baseline (corresponding to the trap center) and the bead being able to freely move away from the coverslip surface when the trap was turned off at the conclusion of the trace. Other examples are given in Figure S1 (Supporting Information). These experiments demonstrate our core–shell particles functionalized with NM monomer can be used in high-force assays to study the mechanics of individual amyloid fibers, and the streptavidin-coated microparticles can easily be implemented into well-established biophysical assays.

To further demonstrate the capabilities of biofunctionalized core–shell beads, an actin rupture assay was performed. Actin is a major cytoskeletal component that is responsible for much of the structure inside of a cell, and its polymerization drives cell motility.[34] Due to the high levels of load an actin network bears in the cell, investigation of its mechanical properties would yield biophysical insight into the cell's force balance mechanisms. The tensile strength of actin has been investigated previously using a pair of glass microneedles,[16,35,36] microfabricated cantilevers,[37] and optical tweezers under low force (0–8 pN).[38] Kishino and Yanagida ruptured an actin filament

© 2018 WILEY-VCH Verlag GmbH & Co. KGaA, Weinheim

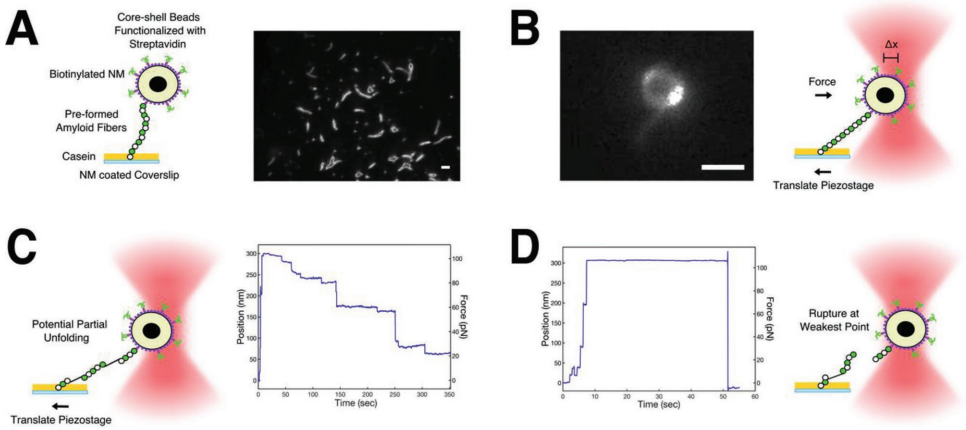

Figure 5. Amyloid pulling assay using core–shell particles. A) Core–shell particles were tethered to a coverslip surface by an amyloid fiber as described previously.[3,4] NM monomers were nonspecifically bound to a coverslip, which was subsequently coated in casein. Pre-formed fluorescent fibers were then added to the flow cell and self-assembled with unfolded monomer on the surface. The fluorescence image shows fibers attached to the surface via monomers (higher concentration than used in pulling assay). Core–shell particles were functionalized with streptavidin using sulfo-SMCC cross-linking and then incubated with biotinylated monomer. B) Beads coated in monomer and fluorescent monomer were used to image an amyloid fiber tethered to the surface. Once a tether was found, the piezostage was translated to generate force on the fiber. C) Unfolding events were observed from pulling on the fiber. As the tether becomes longer from unfolding, the bead drifts back to the trap center. D) After a sustained dwell for more than 40 s, at 100 pN, the tether ruptured. Scale bar: 1 µm.

using glass needles and found the tensile strength to be 108 pN without and 117 pN with tropomyosin, both of which were independent of filament length.[35] Here, core–shell particles were utilized to rupture actin filaments in an optical trapping assay. As shown in **Figure 6**A, core–shells were functionalized with streptavidin, as described earlier, and used to form tethers with single biotinylated actin filaments attached to surface bound streptavidin polystyrene beads (see the Experimental Section). As the phalloidin stabilizer was labeled with Alexa 532, tether formation was confirmed using fluorescence (Figure 6B). Figure 6C shows an example rupture trace of an actin filament using core–shell beads at a trap stiffness of ≈0.3 pN nm^{-1} (see also Figure 3B), with an average rupture force of 90.8 pN ± 26 pN (avg. ± std., $N = 10$). Other examples are given in Figure S2

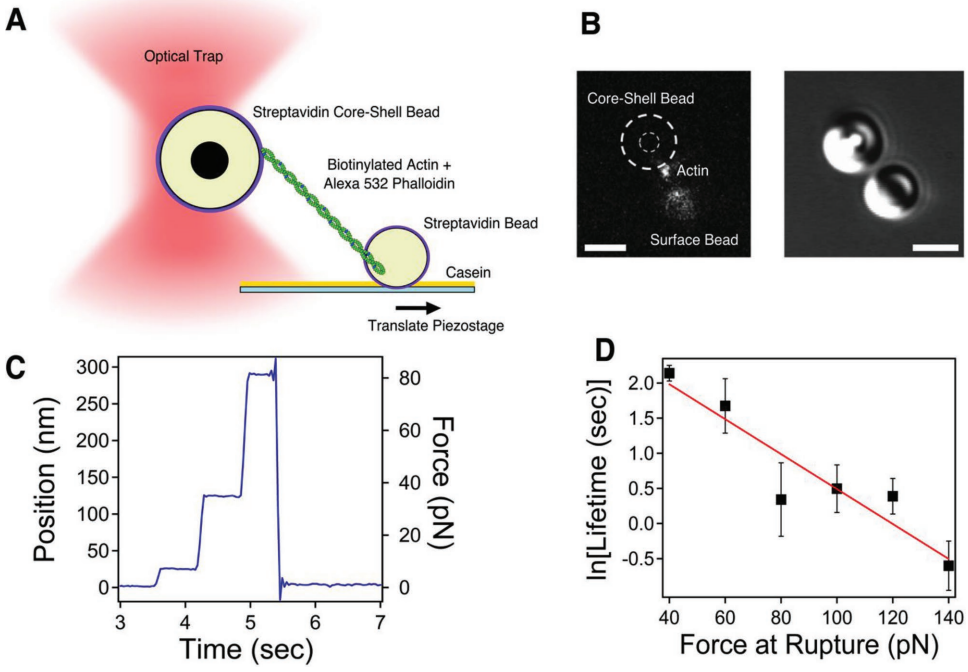

Figure 6. Actin rupture assay. A) Assay schematic. B) Fluorescence visualization of tether formation between a streptavidin-coated core–shell bead and a surface-bound streptavidin bead. Scale bar: 1 µm. C) Example actin rupture trace using beads at a trap stiffness of ≈0.3 pN nm^{-1}. D) Linear relationship between the ln(lifetime) and rupture force, following the Bell model for bond lifetimes.[40] $N = 10$. Error bars: SEM.

© 2018 WILEY-VCH Verlag GmbH & Co. KGaA, Weinheim

(Supporting Information). While it is formally possible that the biotin–streptavidin bond ruptured, it is unlikely in this assay. The biotin–streptavidin rupture force has been reported to be upward of 160 pN,[39] and our lower actin rupture forces are similar to that of Kishino and Yanagida, ≈100 pN.[35] Also, the lifetime of the event (time between total filament elongation and rupture) decreases exponentially with rupture force, following the Bell model for bond lifetimes.[40] While more extensive analysis of actin strength is required, this assay demonstrates core–shell beads' ability to be utilized in high-force biological experiments.

3. Conclusions

Here, we provide a synthetic strategy for making optical trapping handles that display increased trapping stability, detailing how to control the size and refractive index. These handles are composed of a high-refractive-index anatase cores coated with an antireflection titania shell. By introducing a silane functionalizer to the particle surface, we provide a straightforward method for covalently coupling protein structures. We anticipate this approach will broaden the use of these next-generation trapping handles in experiments probing mechanically stable biological interactions/structures, such as studying the mechanics of amyloid fibrils or other high-force experiments previously not possible with an optical trap. Furthermore, these particles are promising candidates for use in combined optical trapping and fluorescence approaches where decreasing trapping laser intensity, without sacrificing trapping stiffness, can provide longer fluorophore lifetimes.[18]

4. Experimental Section

Core–Shell Microparticle Synthesis: The synthetic strategy used in this paper is outlined in Figure 1, based on Jannasch et al.[17] High-refractive-index cores are necessary to increase trapping stability of the final particles. To make the titania cores, a 0.46% (by weight) solution of TBT was chelated with ethylene glycol (EG) overnight in a nitrogen environment under rotation. Specifically, a mixture of 154 µL TBT and 30 mL EG was made in a 60 mL cleaned and dried glass jar inside a nitrogen glove box. The glove box is necessary because the reagents are water sensitive, and the addition of water severely alters the core synthesis. Before the jar was closed, a stir bar was added, and the jar was parafilmed multiple times before removing it from the glove box to mix overnight at ambient conditions. It should be noted that if it is necessary to bring micropipettes and tips into the glove box, the tips should not be attached to the micropipette. Any residual trapped air in the tip can lead to misshapen cores or no core formation; therefore, they must be fully purged with nitrogen as with everything else. Also, cutting off the pipette tip at approximately the first graduated line to make the opening larger aids greatly in accurately pipetting viscous liquids in this protocol (such as TBT and Tween-20).

A 2.03×10^{-3} M Tween-20 solution in 100 mL of acetone was made and rigorously stirred for 10 min. Then, 100 µL of water was added to this solution. The amount of water is crucial for the spherical shape of the cores. Subsequently, the acetone solution was mixed with 18–20 mL of the TBT-EG solution, depending on the size of cores needed (19 mL of TBT-EG solution produced ≈500 nm cores, Figure 2B). Adding more or less TBT-EG will make the cores bigger or smaller, respectively. The reaction mixture was stirred for 10 min to allow for the initial formation of precipitate, the magnetic stir bar was removed, and the solution was stored at room temperature for 24 h. The relatively transparent solution turned into a milky white solution, then forming a precipitate at the bottom of the jar. The particles were collected by centrifuging the solution for 5 min at 7000 rpm and redispersed in cold ethanol stored at 4 °C a total of three times. After the final centrifugation step, the pellet was dried in a microcentrifuge tube in a convection oven at 70 °C for 30 min to evaporate any remaining solvent prior to calcination. The dried cores were then annealed for 1 h at 500 °C in a furnace (Blue M, M15A-1A) to induce a transition of the titania into the anatase phase. Conversion of the cores into the anatase phase was verified using Raman spectroscopy (Renishaw inVia) at 532 nm.[41,42] The cores were sized using a light microscope with DIC. ImageJ[43] was used to analyze the size of the cores in pixels. A pixel to nm conversion can be formed by sizing a distribution of beads with a known size, for example, 0.44, 0.75, and 1.25 µm beads sold by Spherotech. The annealed cores can be stored at room temperature in a sealed container overnight.

The next step is to add shells, which enable the redirection of light in two stages such that an effectively higher refractive index particle is produced. The shells will also be chemically functionalized for biocompatibility. For the addition of the amorphous titania shells, 0.5 mg of anatase cores were resuspended in 3.3 mL of cold ethanol with 800×10^{-6} M Lutensol and disaggregated using a probe sonicator. Separately, a solution of 3.3 mL ethanol and 50–175 µL of TBT was prepared in a glove box under a nitrogen environment in a clean glass jar with a lid. It is essential that the ethanol have no contaminants, such as water or other organic solvents. Thus, the glove box should be purged prior to each use to ensure that trace amounts of organic solvents from other users were removed. Outside the glove box, the core dispersion solution was quickly added to the TBT solution to lessen contact with humid air. The jar was then parafilmed multiple times. The amount of TBT added in this step dictates the diameter of core–shell particles after mixing, with 100 µL TBT producing core–shell particles with diameter ≈1350 nm. The core–TBT mixture was reacted for a total of 2 h in a temperature-controlled bath sonicator at ≈30 °C. The water level in the sonicator should be maintained below the lip of the jar to ensure that no water enters the reaction. Ice can be added to the bath every 10 min if heating occurs from constant sonication, as this can affect the integrity of the parafilm. To incorporate surface-exposed thiol groups, 80 µL of a 1:100 dilution of MPTS in ethanol was added to the reaction mixture after 1 h of sonication. The MPTS solution was prepared under a nitrogen environment in a glove box. Upon completion of the 2 h reaction, the core–shell particles were cleaned by centrifuging for 5 min at 5000 rcf, resuspending in 3 mL of cold ethanol after each wash for a total of three times. After the final wash, the particles were sonicated for 2 min prior to heating. It is important to sonicate the core–shell particles prior to storage or any use as they will clump over time.

The refractive index of the shell can be altered and optimized by heating. Longer heating times result in higher refractive index and concomitantly smaller particles. To tune the index of refraction of the titania shell, a 100 µL aliquot of the cleaned core–shells was centrifuged for 5 min at 1500 rcf in a microcentrifuge tube, and the supernatant was removed. The pellet was resuspended in 10 µL of cold ethanol and sonicated for 2 min. The aliquot was then spun down in a minicentrifuge for a few seconds, and the supernatant was removed. The pellet was heated at 50 °C on a dry block heater for 5–15 min. The particles were then quenched by placing the microcentrifuge tube on ice for 1 min, followed by resuspension of the particles in 100 µL of phosphate buffered saline buffer (137×10^{-3}M NaCl, 2.7×10^{-3} M KCl, 10×10^{-3} M Na_2HPO_4, 2×10^{-3} M KH_2PO_4, pH = 7.4), sonicated for 2 min, and stored at 4 °C under rotation. The final diameter of the core–shells particles was determined similar to the sizing process described for the anatase cores.

Covalent Cross-Linking to Protein or DNA: A two-step cross-linking reaction was used to covalently couple amine-containing proteins to the surface-exposed sulfhydryl groups of the particles. The procedure described here is for the Sup35 prion protein[3] harboring a terminal amine group opposite a C-terminal biotin tag. However, the methodology

© 2018 WILEY-VCH Verlag GmbH & Co. KGaA, Weinheim

is applicable to any biomolecule with a surface-exposed primary amine moiety, such as a DNA strand with a terminal amine.

A 30 µL solution of 100×10^{-6} M protein in PBS was incubated with 3 µL of 20×10^{-3} M sulfo-SMCC, a heterobifunctional cross-linker, at room temperature for 2 h. During the incubation period, 25 µL of core–shell particles were cleaned in 500 µL of PBS containing 0.1% Tween-20 (PBST) by centrifuging at 1500 rcf for 2 min, resuspended in 100 µL of PBS, and sonicated for 2 min. Excess sulfo-SMCC was removed from the protein or DNA solution using a disposable desalting chromatography column (Micro Bio-Spin, Biorad) in PBS buffer a total of three times. The maleimide-activated protein or DNA was then immediately added to the core–shell suspension and mixed overnight at 4 °C. The biofunctionalized core–shells were then washed three times at 1500 rcf for 2 min, and stored in 100 µL of PBST buffer under rotation at 4 °C until use.

Optical Trapping and TIRF: The core–shell particles were tested using a custom-built optical trapping instrument.[44] The optical trapping instrument relies on back focal plane detection of scattered photons for position detection. To quantify any improvement in trapping stability when using core–shells versus commercially available polystyrene particles, the trapping and detection lasers were first aligned, and the trap stiffness was calculated using an equipartition-based calibration (outlined in multiple papers referenced here).[1,45,46] For each batch of core–shells the variance of at least five beads was measured.

To measure the presence of covalently linked proteins on the bead surface using fluorescence, a custom-built TIRF microscope with a 532 nm excitation laser (World Star Technologies) was used for excitation of the Sup35 proteins labeled with Alexa555. Fluorescence emission was imaged using an EM-CCD camera (Andor Technologies).

Amyloid Tethering: To test the functionality of core–shell beads in an inherently high-force assay, tethers were made with amyloid fibers in the same manner as described previously.[3,4] NM monomers (N-terminal and middle domains) from Sup35 prions, fluorescently-tagged NM, and biotinylated-NM were prepared as described previously.[3] Strong-psi (mechanically less strong) NM seeds were used in this study. NM-coated particles were prepared by conjugating streptavidin to thiol-coated particles through the sulfo-SMCC cross-linking reaction. Maleimide–streptavidin was formed by mixing 100 µL of streptavidin (0.5 mg mL^{-1} in PBS) with 2.5 µL sulfo-SMCC (≈23×10^{-3} M in DMSO) and reacted at room temperature for 2 h under rotation. The streptavidin–SMCC mixture was purified using a desalting column equilibrated with CRBB buffer (5×10^{-3} M KPO_4, 150×10^{-3} M NaCl, pH 7.2 + 5×10^{-3} M TCEP). To bind maleimide–streptavidin to thiol-coated particles, 30 µL of maleimide–streptavidin was combined with 200 µL thiol-coated particles. The mixture was incubated for at least 2 h at room temperature or overnight at 4 °C. The particles were then spun down, clarified in CRBB, and gently sonicated for 2 min. To make NM-coated particles, 50 µL streptavidin-coated particles were combined with 1.5 mL biotinylated-NM at 1.2×10^{-3} M and incubated for 1 h at 4°C.

Amyloid fibers were formed as described previously.[3] Briefly, NM fiber solution was made containing 2.5×10^{-3} M NM monomer, fiber seeds, CRBB, and 5×10^{-3} M TCEP. 2.5 mL NM fiber seeds, which are mature NM fibers seeded by yeast cell lysates, were added to 497.5 mL CRBB with 5×10^{-3} M TCEP. NM monomer was added to the solution to make the final concentration of monomer 2.5×10^{-3} M. The sample was briefly vortexed, wrapped with aluminum foil, and incubated at 4 °C for 1 d.

The amyloid pulling assay was assembled similarly as described previously.[3,4] Assembly takes advantage of the fact that the amyloid fiber monomers can be used as handles that fold onto pre-formed amyloid fibers.[3,4] A flow cell was constructed by using a nonetched coverslip and adhering it to a microscope slide with double-sided sticky tape. NM monomers diluted in CRBB buffer (5×10^{-3} M KPO_4, 150×10^{-3} M NaCl, pH 7.2 + 5×10^{-3} M TCEP) at 1×10^{-3} M were added to the flow cell and allowed to incubate for 15 min. The flow cell was then washed with five volumes of CRBB to wash out any unbound monomer. Casein (Blotting-Grade Blocker) at 5 mg mL^{-1} was then added and allowed to incubate for 40 min in order to block any nonspecific binding of future assay components. The flow cell was washed with five volumes of CRBB, and subsequently, pre-formed amyloid fibers were added. After 15 min, the flow cell was washed three times with 1 mL of CRBB + 0.1 mg mL^{-1} casein. Core–shell particles coated in NM monomer were then added to the flow cell and allowed to incubate overnight under high humidity at 4 °C. Before trapping experiments took place, the flow cell was washed three times with 200 mL of CRBB + 0.1 mg mL^{-1} casein to wash out any unbound particles.

For the amyloid pulling experiment, a surface-tethered bead was located on the coverslip surface and subsequently centered in the detection laser, similar to the DNA stretching assay. The optical trap was turned on, and the piezostage was translated to generate force by displacing the bead from the trap center. Bead position and force were measured using custom-written LabVIEW algorithms.

Actin Rupture Experiments: Biotinylated actin (10 actin:1 biotinylated actin) was polymerized as described previously.[47] Briefly, 5 µL 10 mg mL^{-1} actin (Cytoskeleton, AKL99) were mixed with 5 µL 1 mg mL^{-1} biotinylated actin (Cytoskeleton, AB07). General actin buffer (GAB, 5×10^{-3} M Tris-HCl, 0.2×10^{-3}M $CaCl_2$, 0.5×10^{-3} M DTT, 0.2×10^{-3} M ATP) was made, and 100 µL were added to the actin mixture. This mixture was placed on ice for 1 h. Polymerization occurred upon adding 11 µL actin polymerization buffer (APB, 50×10^{-3}M Tris-HCl, 500×10^{-3}M KCl, 2×10^{-3} M $MgCl_2$, 2×10^{-3} M $CaCl_2$, 2×10^{-3} M DTT, 5×10^{-3} M ATP) and incubating for 20 min on ice. Actin filaments were stabilized with 5 µL phalloidin with an Alexa 532 tag (Life Technologies, A22282) and incubation in the dark for 1 h on ice. Actin was then diluted 100× in a 10:1 GAB/APB buffer mixture.

For rupture experiments, an ≈15 µL flow cell was constructed using a microscope slide, an etched coverslip, and double-stick tape. Diluted 1.25 µm streptavidin beads (Spherotech, SVP-10-5) were added to the flow cell and incubated for 10 min to permit surface binding. Then, 10 mg mL^{-1} casein in 10:1 GAB/APB was added to remove any unbound beads and to block the remaining surface, allowing it to incubate for 10 min. Next, diluted biotinylated actin was added to the flow cell and incubated for 10 min to allow binding to surface-affixed beads. Finally, diluted streptavidin-coated core–shell particles in 10:1 GAB/APB were added to the flow cell and allowed to incubate for 10 min. Once the slide was loaded onto the trapping microscope, a self-assembled tether was found by finding a core–shell bead in close proximity to a surface-bound streptavidin bead that was not diffusing away. To rupture the filament, the core–shell bead was trapped, and the piezostage was translated in 200 nm increments at 2 µm s^{-1} until the tether was fully elongated to generate force by displacing the bead from the trap center. Single ruptures were identified through clean, uninterrupted breaks to baseline and the bead diffusing away upon release of the trap. Bead position and force were measured using custom-written LabVIEW algorithms.[48]

Supporting Information

Supporting Information is available from the Wiley Online Library or from the author.

Acknowledgements

J.C.C. and D.N.R. contributed equally to this work. The authors would like to thank Susan Lindquist for advice and amyloid fiber materials and Yu-Chuan Ou for assistance with acquiring Raman spectra. This material is based upon work supported by the National Science Foundation Graduate Research Fellowship Program under Grant No. 1445197 (D.N.R.). J.C.C. was supported in part by a GAANN fellowship from the U.S. Department Of Education Under Grant No. P200A090323. This work was also supported, in part, by the Singapore-MIT Alliance for Research and Technology—BioSyM and NSF Grant No. 1330792 (M.J.L.).

 © 2018 WILEY-VCH Verlag GmbH & Co. KGaA, Weinheim

Conflict of Interest

The authors declare no conflict of interest.

Keywords

biophysics, core–shell particles, force spectroscopy, high force, optical trap

Received: November 30, 2017
Published online: January 15, 2018

[1] K. C. Neuman, S. M. Block, K. C. Neuman, S. M. Block, *Rev. Sci. Instrum.* **2004**, *75*, 2787.
[2] F. M. Fazal, S. M. Block, *Nat. Photonics* **2011**, *5*, 318.
[3] J. Dong, C. E. Castro, M. C. Boyce, M. J. Lang, S. Lindquist, *Nat. Struct. Mol. Biol.* **2010**, *17*, 1422.
[4] C. E. Castro, J. Dong, M. C. Boyce, S. Lindquist, M. J. Lang, *Biophys. J.* **2011**, *101*, 439.
[5] J. P. Mills, D. J. Quinn, M. Dao, M. J. Lang, K. S. W. Tan, C. T. Lim, G. Milon, P. H. David, S. Bonnefoy, S. Suresh, *Proc. Natl. Acad. Sci. USA* **2007**, *104*, 9213.
[6] Y. Hu, T. A. Nieminen, N. R. Heckenberg, H. Rubinsztein-dunlop, *J. Appl. Phys.* **2008**, *103*, 93119.
[7] A. Van Der Horst, P. D. J. Van Oostrum, A. Moroz, A. Van Blaaderen, M. Dogterom, *Appl. Opt.* **2008**, *47*, 3196.
[8] M. Bugiel, H. Fantana, V. Bormuth, A. Trushko, F. Schiemann, J. Howard, *J. Biol. Methods* **2015**, *2*, 1.
[9] M. J. Schnitzer, K. Visscher, S. M. Block, *Nat. Cell Biol.* **2000**, *2*, 718.
[10] J. M. Ferrer, H. Lee, J. Chen, B. Pelz, F. Nakamura, R. D. Kamm, M. J. Lang, *Proc. Natl. Acad. Sci. USA* **2008**, *105*, 9221.
[11] M. D. Wang, H. Yin, R. Landick, J. Gelles, S. M. Block, *Biophys. J.* **1997**, *72*, 1335.
[12] D. E. Smith, S. J. Tans, S. B. Smith, S. Grimes, D. L. Anderson, C. Bustamante, *Nature* **2001**, *413*, 748.
[13] H. Lee, J. M. Ferrer, M. J. Lang, R. D. Kamm, *Phys. Rev. E: Stat. Nonlinear, Soft Matter Phys.* **2010**, *82*, 20.
[14] J. P. Rich, J. Lammerding, G. H. McKinley, P. S. Doyle, *Soft Matter* **2011**, *7*, 9933.
[15] K. C. Neuman, A. Nagy, *Nat. Methods* **2008**, *5*, 491.
[16] H. Kojima, A. Ishijima, T. Yanagida, *Proc. Natl. Acad. Sci. USA* **1994**, *91*, 12962.
[17] A. Jannasch, A. F. Demirors, P. D. J. Van Oostrum, A. Van Blaaderen, E. Schaffer, *Nat. Photonics* **2012**, *6*, 469.
[18] E. J. G. Peterman, F. Gittes, C. F. Schmidt, *Biophys. J.* **2003**, *84*, 1308.
[19] V. Ferro, A. Sonnberger, M. K. Abdosamadi, C. Mcdonald, E. Schaffer, D. McGloin, *Proc. SPIE* **2016**, *9922*, 1.
[20] D. Craig, A. Mcdonald, M. Mazilu, H. Rendall, F. Gunn-moore, K. Dholakia, *ACS Photonics* **2015**, *2*, 1403.
[21] M. J. Lang, P. M. Fordyce, S. M. Block, *J. Biol.* **2003**, *2*, 6.1.
[22] P. B. Tarsa, R. R. Brau, M. Barch, J. M. Ferrer, Y. Freyzon, P. Matsudaira, M. J. Lang, *Angew. Chem.* **2007**, *46*, 1999.
[23] M. A. Van Dijk, L. C. Kapitein, J. Van Mameren, C. F. Schmidt, E. J. G. Peterman, *J. Phys. Chem. B* **2004**, *108*, 6479.
[24] M. H. Stenzel, *ACS Macro Lett.* **2013**, *2*, 14.
[25] H. K. Yu, G. Yi, J. Kang, Y. Cho, V. N. Manoharan, D. J. Pine, S. Yang, *Chem. Mater.* **2008**, *20*, 2704.
[26] A. F. Demirors, A. Jannasch, P. D. J. Van Oostrum, E. Schaffer, A. Imhof, A. Van Blaaderen, *Langmuir* **2011**, *27*, 1626.
[27] A. F. Demirors, A. van Ballderen, A. Imhof, *Chem. Mater.* **2009**, *21*, 979.
[28] B. Bharti, J. Meissner, S. H. L. Klapp, G. H. Findenegg, *Soft Matter* **2014**, *10*, 718.
[29] A. Ashkin, *Biophys. J.* **1992**, *61*, 569.
[30] R. M. Simmons, J. T. Finer, S. Chu, J. A. Spudich, *Biophys. J.* **1996**, *70*, 1813.
[31] M. Schleeger, C. C. vandenAkker, T. Deckert-Gaudig, V. Deckert, K. P. Velikov, G. Koenderink, M. Bonn, *Polymer* **2013**, *54*, 2473.
[32] M.-E. Aubin-Tam, A. O. Olivares, R. T. Sauer, T. A. Baker, M. J. Lang, *Cell* **2011**, *145*, 257.
[33] D. B. Ritchie, M. T. Woodside, *Curr. Opin. Struct. Biol.* **2015**, *34*, 43.
[34] A. Mogilner, G. Oster, *Biophys. J.* **1996**, *71*, 3030.
[35] A. Kishino, T. Yanagida, *Nature* **1988**, *334*, 74.
[36] Y. Tsuda, H. Yasutake, A. Ishijima, T. Yanagida, *Proc. Natl. Acad. Sci. USA* **1996**, *93*, 12937.
[37] X. Liu, G. H. Pollack, *Biophys. J.* **2002**, *83*, 2705.
[38] D. E. Dupuis, W. H. Guilford, J. Wu, D. M. Warshaw, *J. Muscle Res. Cell Motil.* **1997**, *18*, 17.
[39] E. Florin, V. T. Moy, H. E. Gaub, *Science* **1994**, *264*, 415.
[40] G. I. Bell, *Science* **1978**, *200*, 618.
[41] T. Ohsaka, F. Izumi, Y. Fujiki, *J. Raman Spectrosc.* **1978**, *7*, 321.
[42] W. F. Zhang, Y. L. He, M. S. Zhang, Z. Yin, Q. Chen, *J. Phys. D: Appl. Phys.* **2000**, *33*, 912.
[43] C. A. Schneider, W. S. Rasband, K. W. Eliceiri, *Nat. Methods* **2012**, *9*, 671.
[44] W. R. Hesse, M. Steiner, M. L. Wohlever, R. D. Kamm, W. Hwang, M. J. Lang, *Biophys. J.* **2013**, *104*, 1969.
[45] M. J. Lang, C. L. Asbury, J. W. Shaevitz, S. M. Block, *Biophys. J.* **2002**, *83*, 491.
[46] D. C. Appleyard, K. Y. Vandermeulen, H. Lee, M. J. Lang, *Am. J. Phys.* **2007**, *75*, 5.
[47] D. a. Balikov, S. K. Brady, U. H. Ko, J. H. Shin, J. M. de Pereda, A. Sonnenberg, H.-J. Sung, M. J. Lang, *Nucleus* **2017**, *1034*, 1.
[48] A. S. Khalil, D. C. Appleyard, A. K. Labno, A. Georges, M. Karplus, A. M. Belcher, W. Hwang, M. J. Lang, *Proc. Natl. Acad. Sci. USA* **2008**, *105*, 19246.

 © 2018 WILEY-VCH Verlag GmbH & Co. KGaA, Weinheim